We thank Referee #1 for the careful manuscript reading. Below we will address the individual comments.

COMMENT:
Ice nucleating particles can be pre-activated when they are involved in ice nucleation or exposed to low temperatures and high RH. The latter case is investigated in this study assuming that pre-activation occurs by pore condensation and freezing. If pores of aerosol particles are filled with water below 100 % RH with respect to ice, this water can freeze at T < 237 K homogeneously without producing an ice cloud. If the ice within the pores is preserved upon heating, it can induce ice nucleation at T > 237 K. Wagner et al. investigate this mechanism of ice nucleation for a series of INPs, namely two types of zeolites, illite NX, diatomaceous earth, GSG soot, several desert dusts and a volcanic ash sample. Samples were activated by cooling them to 228 K while keeping the relative humidity at constant 95 % with respect to ice. Pre-activation occurred for temperatures up to 260 K for illite, the zeolite samples, GSG soot, diatomaceous earth and one natural dust sample from the Canarian Islands. This ice nucleation behavior was in accordance with pore condensation and freezing assuming pores with diameters from 5 – 8 nm. For smaller pores the ice in the pores is supposed to melt below the ice freezing temperature. Freezing is limited to T < 260 K because larger pores remain empty with the applied pre-activation procedure. The experiments were well designed and conclusively discussed. The results are clearly presented. The paper is well suited for Atmospheric Chemistry and Physics and strongly recommended for publishing. Some minor revisions are suggested:

Page 29004, line 5: WELAS is usually written in capital letters.

ANSWER:
Name will be changed to capital letters.

COMMENT:
Page 29011, line 18: delete “but”

ANSWER:
We wanted to state that the pre-activation has almost disappeared, so we will replace “all but “ by “almost”.

COMMENT:
Figure 5: This Figure should be explained better. It does not become clear how the positions of points in panels A and B are related to each other. Do they refer to the pre-activation cycle over night with constant RHice = 95 %? If yes, this should be stated explicitly. Why is point A missing in panel C? Why are points C, D, and D* missing in panel B?

ANSWER:
In addition to a better explanation, we have also revised Fig. 5 to illustrate the different stages of the pre-activation experiments and their analysis more clearly. The revised version is shown here:

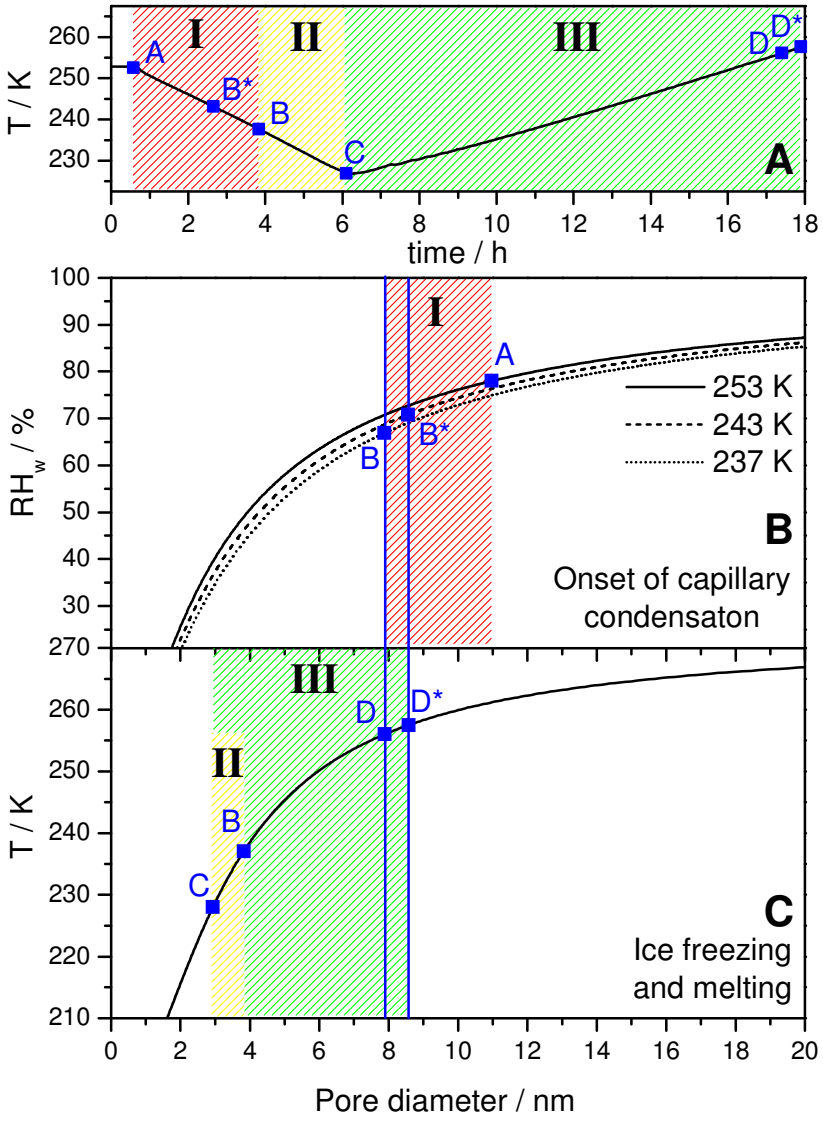

In panel A, we use a colour coding to illustrate the three different processes/stages of the experiment. The red-hatched area (period I) addresses the capillary condensation of supercooled water when the AIDA chamber is cooled from 253 to 237 K with constant RH_{ice} = 95%. This process is analysed in panel B based on the negative Kelvin effect. To simplify panel B, we only show the negative Kelvin curves for three different temperatures in contrast to the four curves shown in the previous version.

Process II is the freezing of the liquid in the pores when cooling the AIDA from point B to point C, which is analysed by the temperature-dependent pore ice stability curve shown in panel C. The same curve applies for describing the melting of ice in the pores when again increasing the AIDA temperature from point C to points D/D* (period III).

With this new graphical representation, it becomes clear why only certain points of the experiments are plotted in panels B and C. The initial cooling period from A to B* and B is analysed by the negative Kelvin effect and the respective points are therefore only shown in panel B. Process III is analysed in panel C and the respective points C, D, D* are therefore only shown there and not in panel B.

Following the suggestions from Referee #2, we have also significantly extended the description of the three processes and how they set the size boundaries of the pores in Sect. 4.1, before details of the computations are addressed in the three subsections 4.1.1, 4.1.2, and 4.1.3. Our revised section 4.1 is as follows (changes highlighted in red):

4.1 Overview: Theoretical considerations on the water condensation, freezing, and melting of ice in pores

Fig. 5A shows the time series of the AIDA temperature during a typical pre-activation experiment. We have used a colour coding to discriminate between the three individual processes that have to be considered for the interpretation of the observed pre-activation behaviour. Process I (red-hatched area) is the capillary condensation of supercooled water when the AIDA chamber is cooled from 253 K (starting temperature for aerosol injection, point A) to 237 K (homogeneous freezing temperature of supercooled water, point B). Process II (yellow-hatched area) is the freezing of capillary-held water when the AIDA temperature is further reduced from 237 to 228 K (point C). Finally, process III (green-hatched area) is the melting of ice in the capillaries when again increasing the temperature of the AIDA chamber. The humidity and temperature conditions for the occurrence of these three processes depend on the pore diameter. Process I is quantitatively analysed based on the negative Kelvin equation that determines the onset of capillary condensation as a function of the pore size (Fig. 5B). This sets a maximum pore dimension for which condensation is just possible at the prevailing RH_w in the AIDA chamber. Process II is analysed based on the temperature-dependent pore ice stability curve (Fig. 5C), which is derived from the critical embryo size for homogeneous ice nucleation as defined in Classical Nucleation Theory. This sets a minimum pore dimension for which freezing of the liquid is possible at the given AIDA temperature. The same curve (Fig. 5C) applies for process (III), the melting of ice in the pores. This analysis yields the maximum temperature for which the pre-activation ability by the PCF mechanism can still be observed in the AIDA chamber. In the following three sections, we outline the details of our calculations.

4.1.1 Process I: Capillary condensation of supercooled water

The concavity of the water surface in a pore results in a Kelvin effect that is inverse compared to a convex liquid droplet, meaning that water condensation can already occur at $RH_w < 100\%$ (Sjogren et al., 2007). Quantitatively, this is taken into account by adding a minus sign to the argument of the exponential of the Kelvin equation (Eq. 1).

$$\frac{e_w}{e_{sat,w}} = \exp\left(-\frac{2M_w\sigma_{w/a}}{RT\rho_w a}\right) \quad (1)$$

Eq. (1) describes the reduction of the saturation water vapour pressure over a concave water meniscus, e_w, in relation to that over a flat water surface, $e_{sat,w}$ (Pruppacher and Klett, 1997). The quotient $e_w/e_{sat,w}$ equals the saturation ratio of moist air with respect to a plane water surface. M_w is the molecular weight of water, $\sigma_{w/a}$ the surface tension for a water-humid air interface, R the universal gas constant, ρ_w the density of water, T the absolute temperature, and a the radius of curvature of the water surface in a capillary. For a circular capillary, a is equal to $D/(2\cos\Theta)$, where D is the pore diameter and Θ the contact angle between water and the pore wall (Fukuta, 1966). In the case of fully wettable capillaries with a zero contact angle, the radius of curvature is equal to the pore radius.

As shown by Marcolli (2014), the measured onset relative humidities for the capillary condensation of water in pores of different mesoporous materials can adequately be described by Eq. (1). We have therefore used this equation to calculate the RH_w values for the onset of capillary condensation of supercooled water for three relevant temperatures to predict the upper size limit of pores that can fill with water at the RH_w conditions prevalent in the AIDA chamber (Fig. 5B). We took into account temperature-dependent parameterisations for $\sigma_{w/a}$ and ρ_w given by Pruppacher and Klett (1997), but ignored the Tolman correction for the size dependence of surface tension (Rao and McMurry, 1990) and assumed a zero contact angle.

Point A in Fig. 5B represents the starting point of the experimental trajectory, denoting the prevalent value of RH_w when the aerosol particles were injected into the chamber at a

temperature of 253 K (corresponding to RH_{ice} = 95% at the same temperature). Here, the maximum diameter of fully wettable pores that can fill with water is about 11 nm. When the AIDA chamber is cooled at constant RH_{ice} of 95% to the homogeneous freezing temperature of supercooled water at 237 K (point B), the relative humidity with respect to supercooled water decreases, meaning that water in larger pores evaporates before it can freeze. When approaching 237 K, capillary-held supercooled water will only be retained in pores with diameters smaller than about 8 nm. Homogeneous freezing could then lead to the formation of ice in such sized pores. Ice formation could also involve slightly larger pores, but this would require that the capillary-held water already freezes heterogeneously at a temperature higher than 237 K (e.g. at point B* with T = 243 K). We will further discuss this issue in Sect. 4.1.3.

4.1.2 Process II: Freezing of capillary-held water

In the next step, we analyse the freezing of the capillary-held water when the AIDA temperature is lowered from the homogeneous freezing limit (point B, 237 K) to the minimum temperature of 228 K (point C). In particular, it has to be examined whether the homogeneous (or heterogeneous) freezing of supercooled water is not impeded for narrow pore diameters. Marcolli (2014) has adopted a quantity from Classical Nucleation Theory to describe the freezing and melting of ice in pores, namely the critical embryo size for homogeneous ice nucleation in the pores. Only if the pore dimension exceeds the critical embryo size, the ice embryo has a higher tendency to grow, which reduces the free energy of the system, than to shrink, which increases the free energy (Pruppacher and Klett, 1997). Ice formation should therefore be inhibited in pores where an ice embryo cannot grow beyond the critical embryo size, even if the temperature is below 237 K.

The critical radius of a spherical ice embryo for homogeneous ice nucleation, r_c, for which the Gibbs free energy of embryo formation within the liquid phase has its maximum, is given by (Murray et al., 2012):

$$r_c = \frac{2M_w\sigma_{i/w}}{RT\rho_i \ln\frac{e_{sat,w}}{e_{sat,i}}} \qquad (2)$$

In Eq. (2), $\sigma_{i/w}$ is the interfacial tension between water and the ice embryo, ρ_i the density of ice, and $e_{sat,i}$ the saturation water vapour pressure over a flat ice surface. Using Eq. (2), we have calculated the temperature-dependent pore diameters needed to incorporate a critical ice embryo as $2r_c + 2t$, where t accounts for a non-freezing quasi-liquid layer between pore wall and ice embryo (Marcolli, 2014). In this computation, t was set to 0.6 nm (Marcolli, 2014), temperature-dependent ρ_i values were obtained from the parameterisation given by Pruppacher and Klett (1997), $e_{sat,w}$ and $e_{sat,i}$ were calculated according to the formulations by Murphy and Koop (2005), and $\sigma_{i/w}$ was taken from the fit of measured homogeneous ice nucleation rate coefficients presented by Zobrist et al. (2007).

The result of the computation is shown in Fig. 5C. Regarding our pre-activation experiments, this curve defines the lower threshold size of pores where ice formation due to freezing of capillary-held water can occur at a given temperature. The yellow-hatched area defines the temperature range of process II as defined in Fig. 5A. At 237 K (point B), the minimum pore size threshold for freezing of the liquid is about 4 nm, and it further decreases to about 3 nm at 228 K, the minimum temperature during the experiment (point C). Here, all aerosol particles with pores in the diameter range from 3 to 8 nm therefore have the chance to incorporate ice due to the PCF mechanism even in an ice-subsaturated environment. 3 nm is the minimum pore size in which capillary-held water can freeze, and 8 nm is the maximum pore size in which condensation of supercooled water has been possible. These ice pockets can trigger the depositional ice growth mode when the aerosol particles are directly probed in an expansion cooling experiment started at 228 K. In our pre-activation experiments, however, we want to investigate the survival of such ice pockets and their contribution to depositional ice growth at warmer temperatures. Therefore, we have to consider as the third

important process the melting of ice when increasing the temperature in the pre-activation experiments (process III, green-hatched areas in Figs. 5A and C).

4.1.3 Process III: Melting of ice in pores

For describing the temperature dependence of the melting of ice in pores, the same curve as for the freezing of ice applies (Marcolli, 2014). Once the diameter of a certain pore gets smaller than the critical embryo size during warming, the ice in the pore should melt because shrinkage of the ice phase would lead to a decrease in the free energy of the system. Point D at 257 K (Fig. 5C) therefore denotes the melting temperature of ice in the largest pores in which ice pockets could have been formed via the PCF mechanism in the case of homogeneous freezing at point B. Above that temperature, the pre-activation behaviour should disappear. In the case of heterogeneous freezing at point B*, the temperature threshold for the disappearance of the pre-activation ability could be a few degrees higher (point D*), because ice in larger pores with a higher melting temperature were present. The suggestion of heterogeneous freezing is, however, somewhat speculative because repeatedly a non-freezing layer of bound water next to the pore walls was found. Therefore, it remains unclear whether the material of the pore wall can actually trigger the freezing of the free water in the pore space. Marcolli (2014) summarised several studies where freezing and melting of ice were insensitive to variations of the surface properties of the pore walls. However, heterogeneous freezing could explain some of our observations, as discussed in Sect. 4.2.

Whereas heterogeneous freezing would increase the temperature threshold for the loss of the pre-activation ability, the opposite behaviour would be encountered if the capillaries of the porous materials were only partially wettable. Here, the factor $\cos\Theta$ would be less than unity, meaning that the radius of curvature of the water meniscus would be larger than the pore radius, thereby reducing the Kelvin effect. The maximum pore size for water condensation would diminish, and hence the upper threshold temperature for the disappearance of the pre-activation behaviour would decrease.

Accurate values for the contact angles between water and the pore walls of our investigated particles are not available. Rather low Θ values of equal or less than 30° were found for several clay minerals (Janczuk and Bialopiotrowicz, 1988). In order to estimate the effect of a non-zero contact angle, we have redone our calculations for a contact angle of 30°. This reduces the 8 nm size threshold for capillary condensation at 237 K to about 6.8 nm, yielding 253 K instead of 257 K as the upper temperature for the loss of pre-activation.

COMMENT:
Page 29015, lines 16 – 19: "In the case of heterogeneous freezing at point B*, the temperature threshold for the disappearance of the pre-activation ability could be a few degrees higher (point D*), because ice in larger pores with a higher melting temperature were present." Is it assumed that the cycle is stopped after the pore water has frozen? Otherwise the ice in the pores might evaporate when RH is further decreased?

ANSWER:
After freezing of the liquid, the stability of ice in the pores towards sublimation will be controlled by the relative humidity with respect to ice, RH_{ice}. Even if we had cooled the AIDA chamber to a temperature lower than 228 K in our cycle, RH_{ice} would have been constant at about 95% due to the ice-covered chamber walls in our experiment, so that the pore ice should not have sublimated. Varying RH_{ice} to test the stability of the pore ice, as done in the experiments by Knopf and Koop (2006), would of course be an interesting issue for further studies. We have already mentioned this in our manuscript on page 29020, lines 7 and 8.

Knopf, D. A., and Koop, T., Heterogeneous nucleation of ice on surrogates of mineral dust, J. Geophys. Res. (Atmos.), 111, D12201, doi:10.1029/2005JD006894, 2006.

COMMENT:
Page 29023, lines 7 – 8: "Above 260 K, the ice in the pores melts and the pre-activation of the aerosol particles is lost." It should be mentioned that this statement refers to the applied pre-activation procedure and not to pre-activation in general.

ANSWER:
Yes, we will extend this statement to:

"Above 260 K, the ice in the pores melts and the pre-activation of the aerosol particles by the PCF mechanism (intermediate cooling to 228 K, $RH_{ice} < 100\%$) is lost."

COMMENT:
Page 29023, lines 17 – 19: "Model calculations suggest that the pre-activation ability is linked to pores of a certain dimension with diameters from about 5 to 8 nm." Again, it should be specified that this refers to the investigated pre-activation conditions, namely,

RHice < 100 % and T = 228 K.

ANSWER:
Yes, we will extend also this statement to:
“Model calculations suggest that the pre-activation ability by the PCF mechanism (intermediate cooling to 228 K, RH_{ice} < 100%) is linked to pores of a certain dimension with diameters from about 5 to 8 nm.”

Best wishes,

Robert Wagner and co-authors